Journal of Engineering and Applied Sciences 12 (Special Issue 1): 5767-5776, 2017
ISSN: 1816-949X

Unsteady Hydromagnetic Convective Heat and Mass Transfer Past an Impulsively Started Infinite Vertical Surface with Newtonian Heating in a Porous Medium

[1]M. Sulemana, [2]Y.I. Seini, [1]M.I. Daabo
[1]Faculty of Mathematical Sciences, [2]School of Engineering,
Nyankpala Campus, University for Development Studies, P.O. Box 1350, Tamale, Ghana

Abstract: Unsteady hydromagnetic convective heat and mass transfer flow past an impulsively started infinite vertical surface with Newtonian heating in a porous medium has been studied. The governing differential equations were transformed using suitable dimensionless parameters. The dimensionless equations were solved employing the Laplace transform techniques and results illustrated graphically for the velocity, temperature and concentration profiles. The study concluded that all the controlling parameters had effects on the flow and can be used to control the flow kinematics.

Key words: Hydromagnetic, convective flow, heat transfer, mass transfer, incompressible fluid, Newtonian heating, Laplace transform

INTRODUCTION

Convective heat and mass transfers have been the focus of many researchers due to its numerous applications in engineering and technological processes. Heat and mass transfer occur simultaneously in several processes such as hot rolling, wire drawing, continuous casting, fiber drawing, evaporation of water at surfaces, drying, etc.

Unsteadiness in a flow is caused by time dependent motion of the external stream or by impulsive motion of the external stream. Siegel (1958) studied the unsteady free convection flow past a semi-infinite vertical plate under step-change in wall temperature or surface heat flux using the momentum integral method. He observed that the initial behaviour of the temperature and velocity fields for semi-infinite vertical flat plate is the same for double infinite vertical flat plate. Martynenko *et al.* (1984) extended Siegel research to include a constant temperature of the plate which is also the temperature of the surrounding stationary fluid. However, in many industrial applications, the plate temperature starts oscillating about a non-zero mean temperature.

At high temperatures, heat transfer caused by radiation is very crucial in many industrial applications such as in Rocket Propulsion Systems, Plasma Physics and in Aerothermodynamics. As a result, some researchers have considered radiation effects in convection flows. Das *et al.* (2012) analyzed the radiation effects on flow past an impulsively started infinite isothermal vertical plate using Laplace transform techniques. Das *et al.* (2012) extended his work to include partial slip at the surface of the boundary, temperature dependent fluid viscosity, variable thermal conductivity and non-uniform heat generation and absorption. Seini and Makinde (2013) studied MHD boundary layer flow due to exponential stretching surface with radiation and chemical reaction. A nonlinear velocity term with MHD was present in the temperature equation. It was found that the rate of heat transfer at the surface decreases with increasing values of the transverse magnetic field and the radiation parameter. Ali *et al.* (2014) studied heat transfer boundary layer flow past an inclined stretching sheet in presence of magnetic field. A nonlinear velocity term with MHD was present in the temperature equation. It was found that velocity profile decreases due to increase of magnetic parameter, Prandtl number and Eckert number whilst velocity increases for increasing values of Grashof number.

It must be noted that heat transfer characteristics are dependent on the thermal boundary conditions. Hence, in Newtonian heating, the rate of heat transfer from the boundary surface with finite heat capacity is proportional to the local surface temperature and this process is called conjugate convective flow. This configuration occurs in many engineering devices such as heat exchangers, fins and solar radiation devices. In these cases, it is necessary to consider convective flows with Newtonian heating.

Corresponding Author: M. Sulemana, Faculty of Mathematical Sciences, Nyankpala Campus, University for Development Studies, P.O. Box 1350, Tamale, Ghana

Chaudhary and Jain (2006) studied the unsteady free convection boundary-layer flow past an impulsively started vertical surface with Newtonian heating using the Laplace transform techniques and observed that the increase of Prandtl number results in decrease in temperature distribution. Narahari and Nayan (2011) considered the free convection flow past an impulsively started infinite vertical plate with Newtonian heating in the presence of thermal radiation and mass diffusion. The exact solutions in a closed-form were obtained by the Laplace transform method with an observation that the velocity increased for aiding flows but decreased for opposing flows. Radiation effects on unsteady free convection flow past a vertical plate with Newtonian heating was reported by Das *et al.* (2012). The governing equations were solved numerically by implicit finite difference method of Crank-Nicolson's type. It was observed that the velocity decreases near the plate and increases away from the plate with increasing Prandtl number or radiation parameter. Hussanan *et al.* (2014) studied unsteady boundary layer flow and heat transfer of a Casson fluid past an oscillating vertical plate with Newtonian heating using Laplace transform technique. It was observed that velocity decreases as Casson parameters incresse and the thermal boundary layer thickness increases with increasing Newtonian heating parameter. Hussanan *et al.* (2015) also investigated Soret effects on unsteady MHD mixed convective heat and mass transfer flow in a porous medium with Newtonian heating using Laplace transform technique and observed that the fluid velocity and the concentration increase with increasing values of Soret number. Hussanan *et al.* (2016) studied heat and mass transfer in a micropolar fluid with Newtonian heating. The plate executes cosine type oscillations. Exact solutions were obtained using Laplace transform technique.

Seini (2013) investigated the flow over an unsteady stretching surface with chemical reaction and non-uniform heat source and concluded that the heat and mass transfer rates and the skin friction coefficient increased as the unsteadiness parameter increases and decreased as the space-dependent and temperature-dependent parameters for heat source/sink increase. Abid *et al.* (2014) studied the slip effects on unsteady free convective heat and mass transfer with Newtonian heating using the Laplace transform method and observed that the presence of the slip parameter reduces the fluid velocity. Furthermore, Etwire *et al.* (2015) investigated the MHD thermal boundary layer flow over a flat plate with internal heat generation, viscous dissipation and convective surface boundary conditions.

In the literature, it is obvious that most of the studies focused on radiation effects on convection flows. To the best knowledge of the researchers, heat and mass transfer of unsteady hydromagnetic convection flows with Newtonian in porous medium has not been reported. In the present study, it is proposed to study the unsteady hydromagnetic convective heat and mass transfer flow past an impulsively started infinite vertical plate with Newtonian heating in porous medium.

MATERIALS AND METHODS

Problem formulation: Consider the unsteady hydromagnetic convective heat and mass transfer flow of an optically dense viscous and incompressible fluid past an impulsively started infinite vertical surface with Newtonian heating. Three fluids are considered in this study namely air, electrolyte solution and water. The flow is assumed to be in the x*-axis direction which is taken along the plate in the vertical upward direction and the y*-axis is chosen normal to the plate. At time $t^* \leq 0$, both the fluid and the plate are at rest with a constant temperature and concentration T^*_∞ and C^*_∞, respectively. At time $t^* > 0$, the plate is subjected to an impulsive motion in vertically upward direction against gravitational field with a uniform velocity U_0 and at a temperature T^*_w and the concentration level near the plate is raised to C^*_w. The physical system of the flow is shown in Fig. 1.

Since, the plate is infinitely along the x* direction, all the physical variables are the functions of y* and t* only. Therefore, under the usual Boussinesq approximation and neglecting the inertia terms, viscous dissipation heat Soret and Dufour effects, the flow is governed by Eq. 1-3:

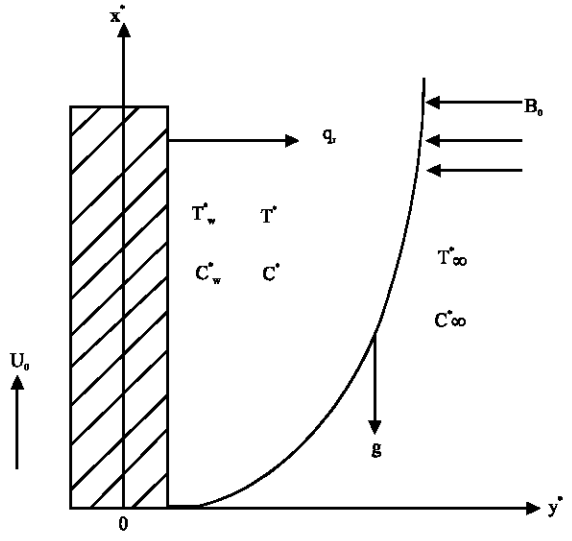

Fig. 1: Flow configuration and coordinate system

$$\frac{\partial u^*}{\partial t^*} = \nu \frac{\partial^2 u^*}{\partial y^{*2}} + g\beta_T (T^* - T_\infty^*) + g\beta_c (C^* - C_\infty^*) - \frac{\sigma B_0^2}{\rho} u^* \quad (1)$$

$$\rho c_p \frac{\partial T^*}{\partial t^*} = k \frac{\partial^2 T^*}{\partial y^{*2}} - \frac{\partial q_r}{\partial y^*} + \sigma B_0^2 u^{*2} \quad (2)$$

$$\frac{\partial C^*}{\partial t^*} = D \frac{\partial^2 C^*}{\partial y^{*2}} - K_C (C^* - C_\infty^*) \quad (3)$$

With boundary conditions:

$$\begin{aligned} &u^* = 0, T^* = T_\infty^* \quad C^* = C_\infty^* \text{ for all } y^* \geq 0, \quad t^* \leq 0 \\ &u^* = U_0, T^* = T_w^*, \; C^* = C_w^* \text{ at } y^* = 0, \quad t^* > 0 \\ &u^* \to 0, \quad T^* \to T_\infty^*, \quad C^* \to C_\infty^* \text{ as } y^* \to \infty, \quad t^* > 0 \end{aligned} \quad (4)$$

Where:

u^* = The horizontal velocity component
U_0 = The velocity of the plate
y^* = The coordinate axis normal to the plate
t^* = The time
ν = The kinematic viscosity
β_T = The volumetric coefficient of the thermal expansion
ρ = The fluid density
T^* = The fluid temperature near the plate
T_∞^* = The temperature of the fluid far away from the plate
T_w^* = The temperature of the plate surface
C^* = The concentration in the fluid
C_∞^* = The concentration far away from the plate
C_w^* = The concentration at the plate surface
k = The thermal conductivity
D = The mass diffusivity
K_C = Dimensionless the rate of chemical reaction
β_C = The concentration expansion co-efficient
q_r = The radiative flux
c_p = The specific heat at constant pressure

The following dimensionless equalities similar to dimensionless parameters used by Narahari and Nayan (2011), Abid *et al.* (2014) and Chaudhary and Jain (2006) are introduced:

$$\begin{aligned} &u = \frac{u^*}{U_0}, \; y = \frac{u_0 y^*}{\nu}, \; \theta = \frac{T^* - T_\infty^*}{T_w^* - T_\infty^*}, \; t = \frac{t^* U_0^2}{\nu}, \; Ec = \frac{u^2}{Cp(T_w^* - T_\infty^*)} \\ &\varnothing = \frac{C^* - C_\infty^*}{C_w^* - C_\infty^*}, \; P_r = \frac{\mu C_p}{k}, \; G_r = \frac{\nu g \beta_T T_\infty^*}{U_0^3}, G_C = \frac{\nu g \beta_c (C_w^* - C_\infty^*)}{U_0^3}, \\ &k_c = \frac{\nu k_c^*}{U_0^2}, \; F = \frac{16\sigma a^* \nu^2 T_\infty^*}{K U_0^2}, \; S_c = \frac{\nu}{D}, \; M = \frac{\sigma B_0^2 \nu}{\rho U_0^2} \end{aligned} \quad (5)$$

Where:

y = The dimensionless coordinate axis normal to the plate surface
u = The dimensionless velocity in x direction
θ = The dimensionless temperature
t = The dimensionless time
k = The dimensionless permeability of porous medium
K_∞^* = The rate of chemical reaction
K_C = The dimensionless rate of chemical reaction
S_C = The Schmidt number
P_r = The Prandtl number
G_r = The thermal Grashof number
G_c = The mass Grashof number
σ = The electrical conductivity
g = The acceleration due to gravity
$\varnothing$ = The dimensionless concentration in the fluid
N = The buoyancy ratio parameter
F = The radiation parameter
μ = The coefficient of viscosity
E_c = The Eckert number

Using the Rosseland approximation:

$$\frac{\partial q_r}{\partial y^*} = -4a^* \sigma (T_\infty^* - T^{*4}) \quad (6)$$

Where:

a^* = The Rosseland mean absorption co-efficient
σ = The Stefan-Boltzmann constant
q_r = The radiative heat flux

Assuming that the temperature differences with the flow are sufficiently small such that T^{*4} is expressed as a linear function of the temperature. By Taylor series expansion neglecting the higher order terms, T^{*4} is expressed as a linear function of the temperature in the form:

$$T^{*4} \approx 4T_\infty^{*3} T^* - 3T_\infty^{*4} \quad (7)$$

Substituting Eq. 7 into Eq. 6:

$$\begin{aligned} \frac{\partial q_r}{\partial y^*} &= -4a^* \sigma (T_\infty^{4*} - 4T_\infty^{*3} T^* + 3T_\infty^{*4}) \\ &= -4a^* \sigma (4T_\infty^{*4} - 4T_\infty^{*3} T^*) \\ &= -16a^* \sigma (T_\infty^{*4} - T_\infty^{*3} T^*) \end{aligned}$$

$$\frac{\partial q_r}{\partial y^*} = -16a^* \sigma T_\infty^{*3} (T_\infty^* - T^*) \quad (8)$$

Substituting Eq. 8 in Eq. 2 and the transformation of Eq. 5 in Eq. 1-3 give the following dimensionless models:

$$\frac{\partial u}{\partial t} = \frac{\partial^2 u}{\partial y^2} + Gr\theta + G_c \varnothing - Mu \quad (9)$$

$$\frac{\partial \theta}{\partial t} = \frac{1}{P_r} \left(\frac{\partial^2 \theta}{\partial y^2} - F\theta \right) + ME_c u^2 \quad (10)$$

$$\frac{\partial \varnothing}{\partial t}=\frac{1}{S_C}\frac{\partial^2 \varnothing}{\partial y^2}-K_C\varnothing \tag{11}$$

Subject to the boundary conditions in dimensionless form:

$$\begin{aligned} &u=0 \quad \theta=0 \; c=0 \text{ for all } y\geq 0, t\leq 0\\ &u=1 \quad \theta=0, \; c=1 \text{ for all } y\; y=0, t>0\\ &u\to 0 \quad \theta\to 0 \quad c\to 0 \text{ as } y\to\infty, \; t>0 \end{aligned} \tag{12}$$

Problem solution: The non-linear differential Eq. 9-11 with boundary conditions (Eq. 12) are solved numerically in exact form using Laplace transform technique.

The energy Eq. 10 and the concentration Eq. 11 are uncoupled from the momentum Eq. 9. Hence, the temperature variable $\theta(y, t)$ and the concentration variable $\varnothing(y, t)$ will be solved upon which the solution of the velocity u(y, t) can be obtained. Using Laplace transform technique, the solutions are derived as:

$$\theta(y,s)=\left(\frac{-ME_C}{s}\right)e^{-\sqrt{s P_r}\,y}+\frac{ME_C}{s} \tag{13}$$

where, s is the Laplace transform parameter. Taking inverse Laplace transform. The general solution for the temperature $\theta(y, t)$ at t>0 is:

$$\theta(y,t)=ME_C\left(\operatorname{erf}\left(\frac{y\sqrt{P_r}}{2\sqrt{t}}\right)\right) \tag{14}$$

$$\varnothing(y,S)=e^{-\sqrt{sS_c}\,y}+k_c\left(\frac{e^{-y\sqrt{S_c}\sqrt{s}}}{s}-\frac{1}{s}\right) \tag{15}$$

Taking inverse Laplace transform. For the concentration, $\varnothing(y, t)$ at t>0, the general solution is:

$$\varnothing(y,t)=\frac{y\sqrt{S_c}\,e^{-y^2S_c/(4t)}}{2\sqrt{\pi t^3}}-k_C\left(\operatorname{erf}\left(\frac{y\sqrt{S_c}}{2\sqrt{t}}\right)\right) \tag{16}$$

$$\begin{aligned} U(y,S)=&\left(1-G_r\theta\frac{1}{s}-G_c\varnothing\frac{1}{s}+M\frac{1}{s}\right)\\ &e^{-y\sqrt{s}}+G_r\theta\frac{1}{s}+G_c\varnothing\frac{1}{s}-M\frac{1}{s} \end{aligned} \tag{17}$$

Taking the inverse Laplace transform:

$$\begin{aligned} U(y,t)=&\frac{ye^{-y^2/(4t)}}{2\sqrt{\pi t^3}}+G_r\theta\left(\operatorname{erf}\left(\frac{y}{2\sqrt{t}}\right)\right)+\\ &G_c\varnothing\left(\operatorname{erf}\left(\frac{y}{2\sqrt{t}}\right)\right)-M\left(\operatorname{erf}\left(\frac{y}{2\sqrt{t}}\right)\right) \end{aligned} \tag{18}$$

Where:

$$\theta(y,t)=ME_c\left(\operatorname{erf}\left(\frac{y\sqrt{P_r}}{2\sqrt{t}}\right)\right)$$

$$\varnothing(y,t)=\frac{y\sqrt{S_c\,e^{-y^2Sc/(4t)}}}{2\sqrt{\pi t^3}}-k_c\left(\operatorname{erf}\left(\frac{y\sqrt{S_c}}{2\sqrt{t}}\right)\right)$$

For the velocity, U(y, t) at t>0, the general solution is:

$$\begin{aligned} U(y,t)=&\left(\frac{ye^{-y^2/(4t)}}{2\sqrt{\pi t^3}}\right)+G_r\left[ME_c\left(\operatorname{erf}\left(\frac{y\sqrt{P_r}}{2\sqrt{t}}\right)\right)\right]\\ &\left(\operatorname{erf}\left(\frac{y}{2\sqrt{t}}\right)\right)+G_c\left[\frac{y\sqrt{S_c\,e^{-y^2S_c/(4t)}}}{2\sqrt{\pi t^3}}-k_c\left(\operatorname{erf}\left(\frac{y\sqrt{S_c}}{2\sqrt{t}}\right)\right)\right]\\ &\left(\operatorname{erf}\left(\frac{y}{2\sqrt{t}}\right)\right)-M\left(\operatorname{erf}\left(\frac{y}{2\sqrt{t}}\right)\right) \end{aligned} \tag{19}$$

Other possible solutions: Since, Prandtl number is the ratio of momentum diffusivity to thermal diffusivity of the fluid, $P_r = 1$ refers to those fluids whose momentum and thermal boundary layer thickness are of magnitude of the same order and the temperature $\theta(y, t)$ solution in (Eq. 26) is valid for all values of P_r except $P_r = 0$ which is not practically possible. The concentration solution $\varnothing(y, t)$ is also valid for all values of S_c except $S_c = 0$ which is rare in practice. Other possible solutions are:

Case 1: When $P_r = 1$ and $S_c = 1$:

$$\begin{aligned} U(y,t)=&\left(\frac{ye^{-y^2/(4t)}}{2\sqrt{\pi t^3}}\right)+G_r\left[ME_c\left(\operatorname{erf}\left(\frac{y}{2\sqrt{t}}\right)\right)\right]\\ &\left(\operatorname{erf}\left(\frac{y}{2\sqrt{t}}\right)\right)+G_c\left[\frac{y\,e^{-y^2/(4t)}}{2\sqrt{\pi t^3}}-k_c\left(\operatorname{erf}\left(\frac{y}{2\sqrt{t}}\right)\right)\right]\\ &\left(\operatorname{erf}\left(\frac{y}{2\sqrt{t}}\right)\right)-M\left(\operatorname{erf}\left(\frac{y}{2\sqrt{t}}\right)\right) \end{aligned}$$

Case 2: When $P_r \neq 1$ and $S_c = 1$:

$$\begin{aligned} U(y,t)=&\left(\frac{ye^{-y^2/(4t)}}{2\sqrt{\pi t^3}}\right)+G_r\left[ME_c\left(\operatorname{erf}\left(\frac{y\sqrt{P_r}}{2\sqrt{t}}\right)\right)\right]\\ &\left(\operatorname{erf}\left(\frac{y}{2\sqrt{t}}\right)\right)+G_c\left[\frac{y\,e^{-y^2/(4t)}}{2\sqrt{\pi t^3}}-k_c\left(\operatorname{erf}\left(\frac{y}{2\sqrt{t}}\right)\right)\right]\\ &\left(\operatorname{erf}\left(\frac{y}{2\sqrt{t}}\right)\right)-M\left(\operatorname{erf}\left(\frac{y}{2\sqrt{t}}\right)\right) \end{aligned}$$

Case 3: When $P_r = 1$ and $S_c \neq 1$:

$$U(y,t)=\left(\frac{ye^{-y^2/(4t)}}{2\sqrt{\pi t^3}}\right)+G_r\left[ME_c\left(erf\left(\frac{y}{2\sqrt{t}}\right)\right)\right]$$
$$\left(erf\left(\frac{y}{2\sqrt{t}}\right)\right)+G_c\left[\frac{y\sqrt{S_c}\,e^{-y^2S_c/(4t)}}{2\sqrt{\pi t^3}}-k_c\left(erf\left(\frac{y\sqrt{S_c}}{2\sqrt{t}}\right)\right)\right]$$
$$\left(erf\left(\frac{y}{2\sqrt{t}}\right)\right)-M\left(erf\left(\frac{y}{2\sqrt{t}}\right)\right)$$

RESULTS AND DISCUSSION

In order to determine the effects of the physical parameters such as t, P_r, S_c, G_r, G_C, M, E_c and K_c on the hydromagnetic convection flow, the numeric values of the temperature, concentration and velocity fields were computed and shown in Fig. 2. Three fluids were considered in this study namely air, electrolyte solution and water. The values of the Prandtl number (P_r) are taken as 0.71 (for air), 1.0 (for electrolyte solution) and 7.0 (for water) and the values of the Schmidt number (S_c) are taken as 0.24 (air), 0.67 (electrolyte solution) and 0.62 (water) which are the physical values of P_r and S_c of these fluids. However, the value S_c = 0.67 (electrolyte solution) is used in the analysis since in electrolyte solutions the S_c is usually large.

Figure 2 shows the effect of the Prandtl number on the temperature profilefor electrolyte solution (P_r = 1.0), air (P_r = 0.71) and water (P_r = 7.0). Although, smaller Prandtl numbers give greater thermal boundary layer thickness (Chaudhary and Jain, 2006; Narahari and Nayan, 2011), however, the presence of the magnetic field delay the convection motion. Since, the molecules of water are closer to each other than air, they get heated or charged up faster than air in the presence of magnetic field hence the reverse process occurred. Therefore, it is observed that the thermal boundary layer thickness is greater for water (P_r = 7.0) as compared to air (P_r = 0.71) and electrolyte solution (P_r = 1.0). Thus, the temperature falls more rapidly for air than water and electrolyte solution. Also, the thermal boundary layer thickness decreases with increase in time.

Figure 3-7 represent the effect of Eckert number E_c on the temperature profile for electrolyte solution (P_r = 1.0), air (P_r = 0.71) and water (P_r = 7.0), respectively. It is observed that as the time passes, the temperature falls for the positive values of E_c whilst for the negative values of Ec the reverse occurred.

Figure 7 Illustrates the effect of the magnetic parameter M on the temperature profile for electrolyte solution (P_r = 1.0), air (P_r = 0.71) and water (P_r = 7.0). It is noticed that the thermal boundary layer thickness

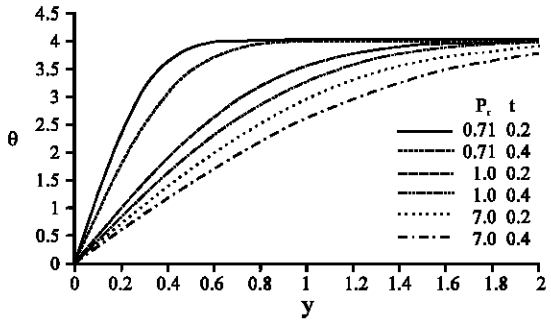

Fig. 2: Temperature profile in the presence of magnetic field for electrolyte solution (P_r = 1.0), air (P_r = 0.71) and water (P_r = 7.0) when M = 2 and E_c = 2

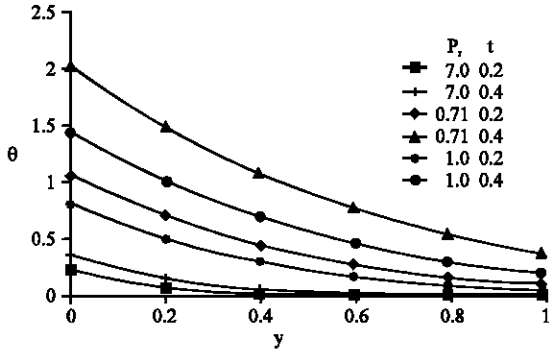

Fig. 3: Temperature profile in the absence of magnetic field (Chaudhary and Jain, 2006)

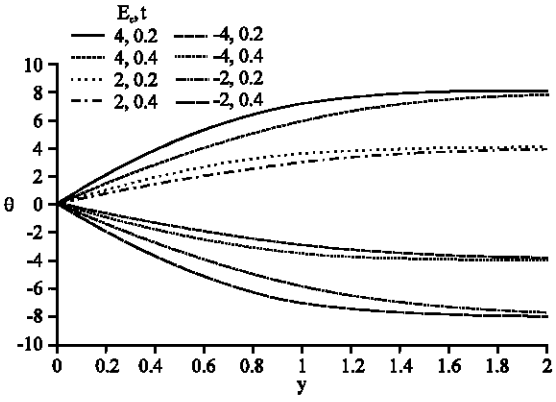

Fig. 4: Temperature profile of the effect of the Eckert number (E_c) on the electrolyte solution (P_r = 1.0) when M = 2

is greater for water (P_r = 7.0) than electrolyte solution (P_r = 1.0) and air (P_r = 0.71) as the magnetic parameter M increases.

Figure 8 shows the effect of the Schmidt number S_c on the concentration profilefor electrolyte solution

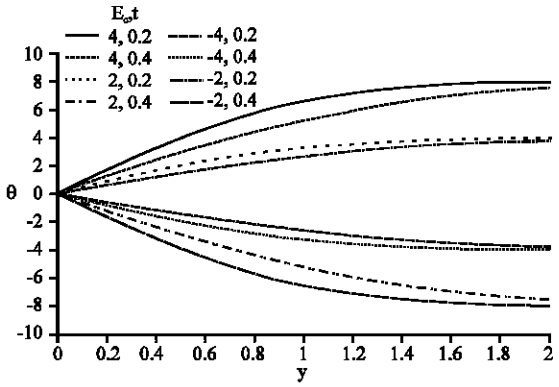

Fig. 5: Temperature profile of the effect of the Eckert number (E_c) on air (P_r = 0.71) when M = 2

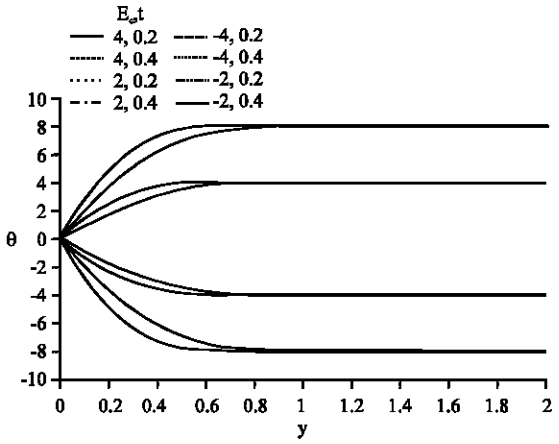

Fig. 6: Temperature profile of the effect of the Eckert number (E_c) on water (P_r = 7.0) when M = 2

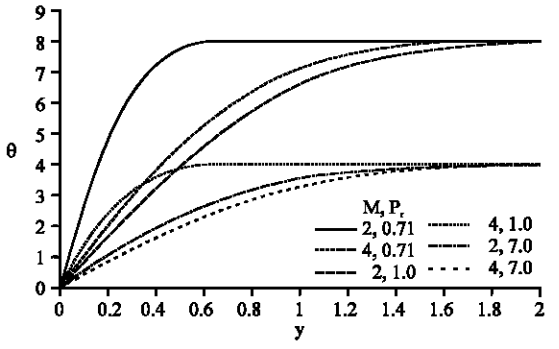

Fig. 7: Temperature profile of the effect of Magnetic parameter M on electrolyte solution (P_r = 1.0), air (P_r = 0.71) and water (P_r = 7.0) when E_c = 2 and t = 0.2

(S_c = 0.67), air (P_r = 0.24) and water (P_r = 0.62). It is realized that concentration is high for electrolyte solution

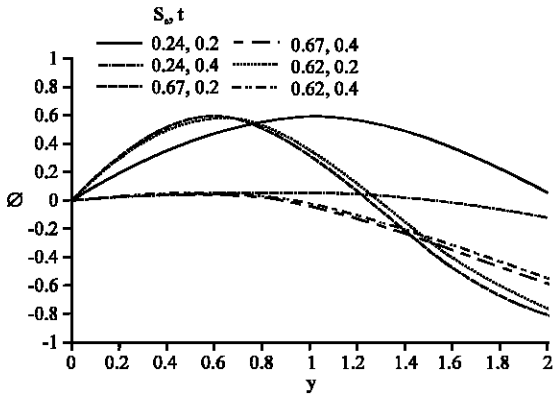

Fig. 8: Concentration profile for air (S_c = 0.24), electrolyte solution (S_c = 0.67) and water (S_c = 0.62) when K_c = 1

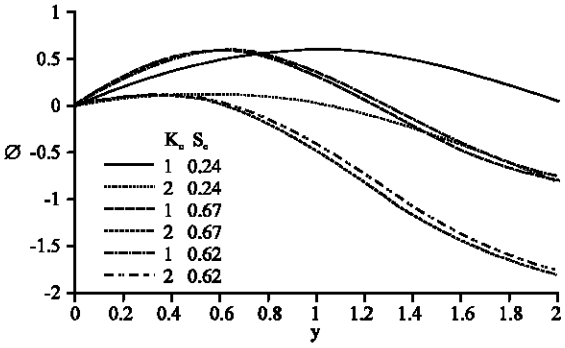

Fig. 9: Concentration profile of the effect of rate of chemical reaction (K_c) on air (S_c = 0.24), electrolyte solution (S_c = 0.67) and water (S_c = 0.62) when t = 0.2

(S_c = 0.67) as compared to water (S_c = 0.62) and air (0.24). However, the concentration decreases faster for electrolyte solution (S_c = 0.67) as compared to water (S_c = 0.62) and air (0.24) as time passes.

Figure 9 shows the effect of rate of chemical reaction K_c on air (S_c = 0.24), electrolyte solution (S_c = 0.67) and water (S_c = 0.62) is considered. Again, concentration is high for electrolyte solution (S_c = 0.67) as compared to water (S_c = 0.62) and air (0.24). Also as time goes on, concentration decreases faster for electrolyte solution (S_c = 0.67) as compared to water (S_c = 0.62) and air (0.24).

Figure 10 illustrates velocity profile for air (Pr = 0.71), electrolyte solution (P_r = 1.0) and water (P_r = 7.0). It is noticed that increase in velocity is greater for water (P_r = 7.0) as compared to electrolyte solution (P_r = 1.0) and air (P_r = 0.71). The velocity however, decreases for all the three fluids as time passes.

Figure 11-16 represent the effect of Grashof number G_r on the velocity profile for electrolyte solution (P_r = 1.0),

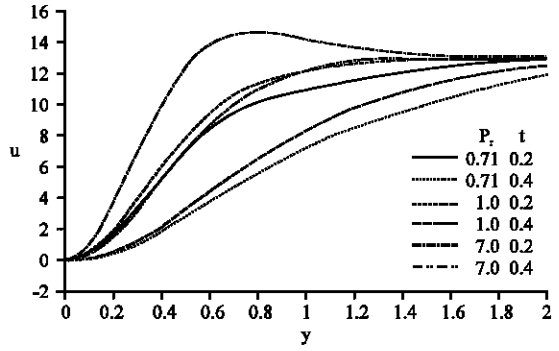

Fig. 10: Velocity profile for air (P_r = 0.71), electrolyte solution (P_r = 1.0) and water (P_r = 7.0) when M = 2, E_c = 2, S_c = 2.01, K_c = 1, G_r = 5, G_c = 5

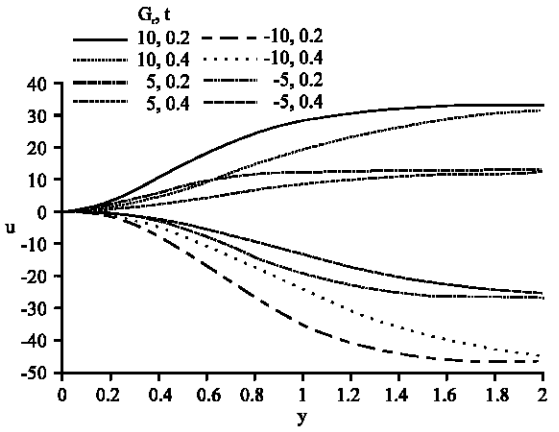

Fig. 11: Velocity profile of the effect of Grashof number G_r on electrolyte solution (P_r = 1.0) with magnetic field when M = 2, E_c = 2, S_c = 2.01, K_c = 1, G_c = 5

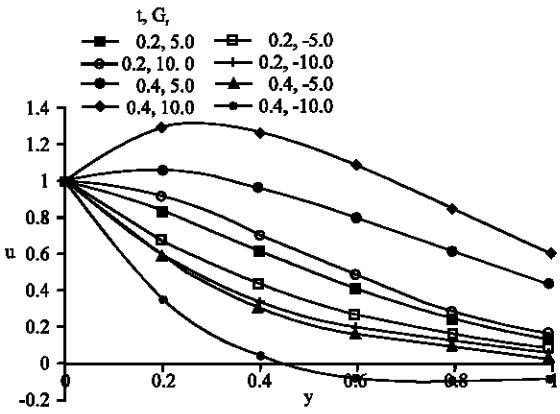

Fig. 12: Velocity profile for electrolyte solution P_r = 1.0 (no magnetic field) (Chaudhary and Jain, 2006)

air (P_r = 0.71) and water (P_r = 7.0), respectively. Though, the effect of an increase in Grashof number is to raise the

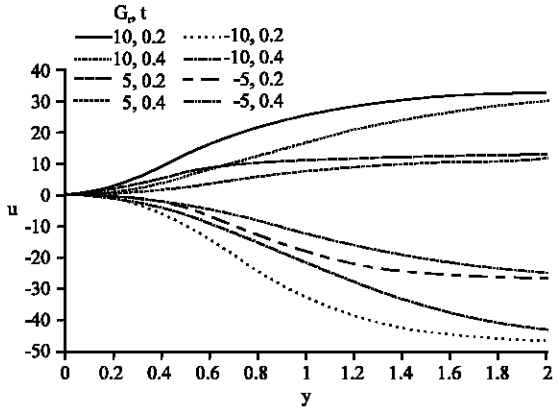

Fig. 13: Velocity profile of the effect of Grashof number G_r on air (P_r = 0.71) with magnetic field when M = 2, E_c = 2, S_c = 2.01, K_c = 1, G_c = 5

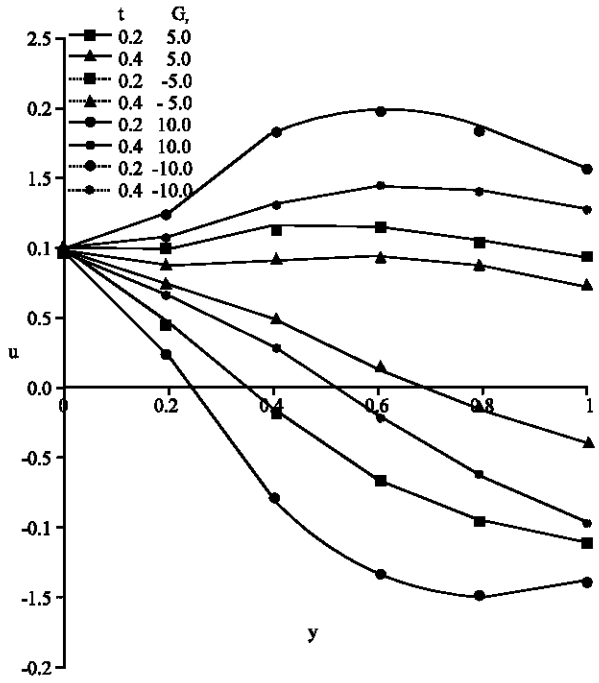

Fig. 14: Velocity profile for air P_r = 0.71 (no magnetic field) (Chaudhary and Jain, 2006)

velocity values. Due to the presence of the magnetic field, it is observed that as time goes on, the velocity decreases for positive values of G_r but increases for negative values of G_r. However, the velocity remains positive for G_r>0 and negative for G_r<0.

Figure 17-19 shows the effect of mass Grashof number G_c on the velocity profile for electrolyte solution (P_r = 1.0), air (P_r = 0.71) and water (P_r = 7.0), respectively. It is noticed that the velocity decreases as time goes on. However, the velocity increases for G_r<0 and decreases for G_r>0.

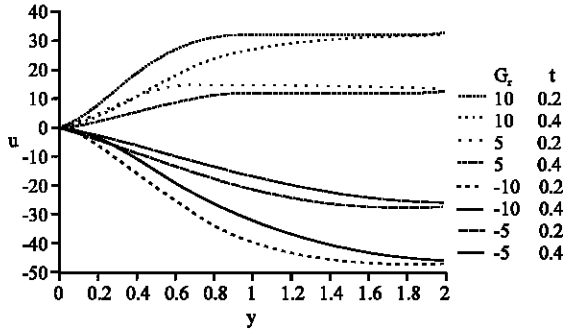

Fig. 15: Velocity profile of the effect of Grashof number G_r on water (P_r = 7.0) with magnetic field when M = 2, E_c = 2, S_c = 2.01, K_c = 1, G_c = 5

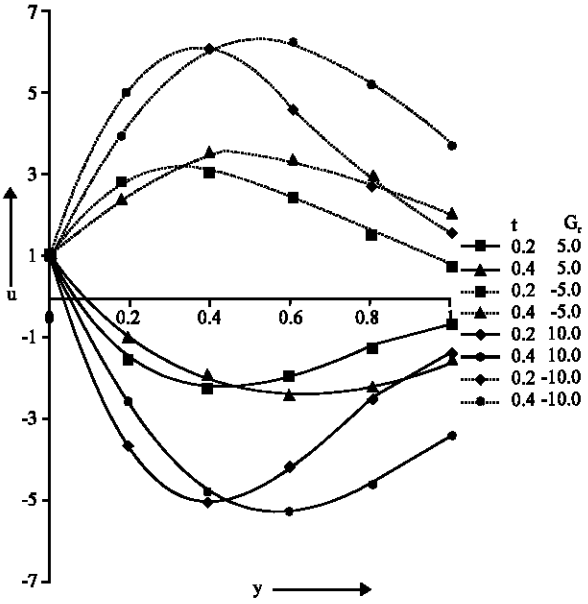

Fig. 16: Velocity profile for water P_r = 7.0 (no magnetic field) (Chaudhary and Jain, 2006)

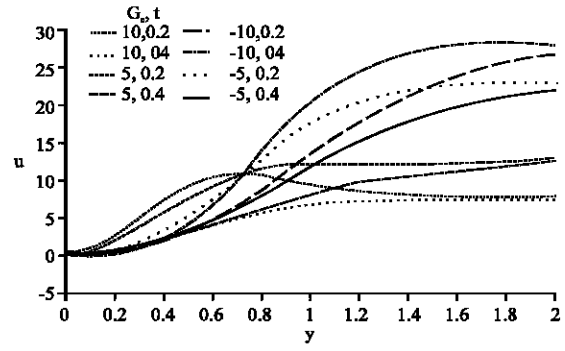

Fig. 17: Velocity profile of the effect of mass Grash of number G_c on electrolyte solution (P_r = 1.0) when M = 2, E_c = 2, S_c = 2.01, K_c = 1, G_r = 5

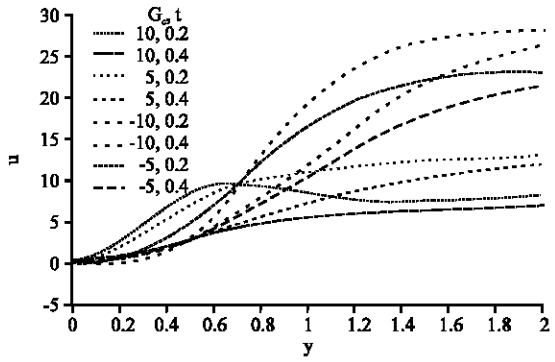

Fig. 18: Velocity profile of the effect of mass Grash of number G_c on air (P_r = 0.71) when M = 2, E_c = 2, S_c = 2.01, K_c = 1, G_r = 5

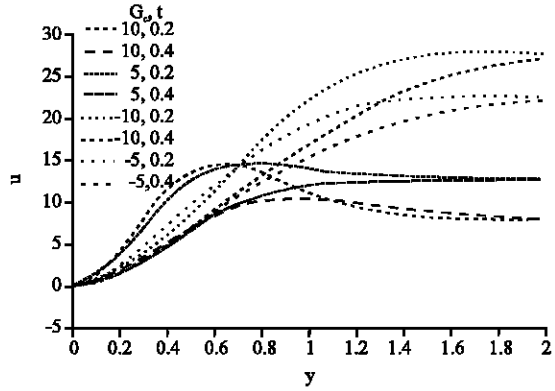

Fig. 19: Velocity profile of the effect of mass Grash of number G_c on water (P_r = 7.0) when M = 2, E_c = 2, S_c = 2.01, K_c = 1, G_r = 5

Figure 20 shwes the effect of the magnetic parameter M on the velocity profile for electrolyte solution (P_r = 1.0), air (P_r = 0.71) and water (P_r = 7.0) is considered. It revealed that the velocity increases for all the three fluids as the magnetic parameter M increases. However, the increase in velocity of water (P_r = 7.0) is greater as compared to air (P_r = 0.71) and electrolyte solution (P_r = 1.0).

Figure 21 illustrates the effect of the Eckert number on the velocity profile for electrolyte solution (P_r = 1.0), air (P_r = 0.71) and water (P_r = 7.0). The velocity increases with increase in Eckert number for all the fluids. However, the velocity increased is greater for water (P_r = 7.0) than air (P_r = 0.71) and electrolyte solution (P_r = 1.0).

Figure 22 shows the effect of the rate of chemical reaction K_c on the velocity profile for electrolyte solution (P_r = 1.0), air (P_r = 0.71) and water (P_r = 7.0) is determined. It is noticed that the velocity decreases with increase in the rate of chemical reaction K_c.

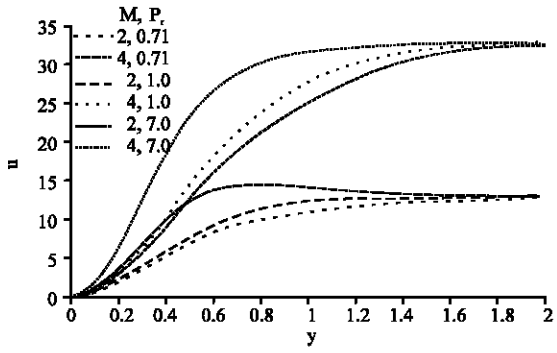

Fig. 20: Velocity profile of the effect of magnetic parameter M on electrolyte solution (P_r = 1.0), air (P_r = 0.71) and water (P_r = 7.0) when E_c = 2, S_c = 2.01, K_c = 1, G_r = 5, G_c = 5

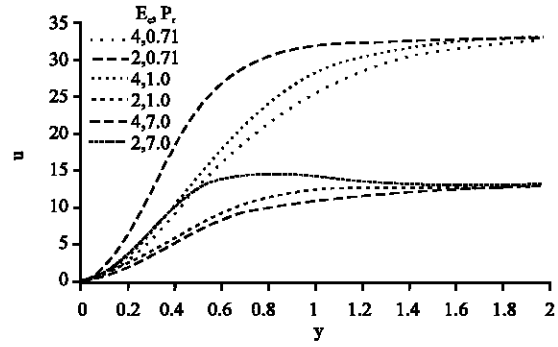

Fig. 21: Velocity profile of the effect of Eckert numberon electrolyte solution (P_r = 1.0), air (P_r = 0.71) and water (P_r = 7.0) when M = 2, S_c = 2.01, K_c = 1, G_r = 5, G_c = 5

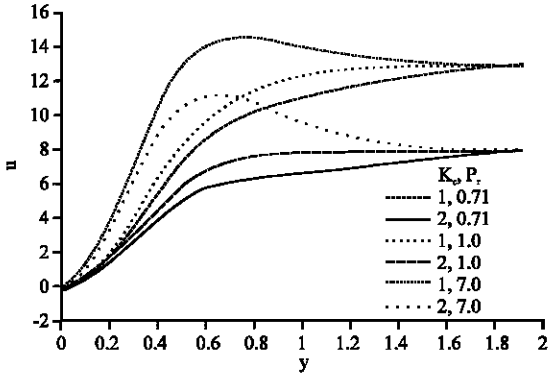

Fig. 22: Velocity profile of the effect of rate of chemical reaction K_c on air (P_r = 0.71), electrolyte solution (P_r = 1.0) and water (P_r = 7.0) when M = 2, E_c = 2, S_c = 2.01, G_r = 5, G_c = 5

CONCLUSION

Unsteady hydromagnetic convective heat and mass transfer flow with Newtonian heating in a porous medium has been investigated. The non-linear partial differential equations have been modeled and transformed to appropriate dimensionless differential equations using suitable dimensionless parameters. The Laplace transform techniques were employed to solve the resulting dimensionless differential equations directly and results showed graphically using MATLAB. From the results obtained, the following conclusions can be drawn: in the presence of magnetic field, the thermal boundary layer thickness is greater for water (P_r = 7.0) as compared to air (P_r = 0.71) and electrolyte solution (P_r = 1.0) but diminishes with time. The concentration is high for electrolyte solution (S_c = 0.67) compared to water (S_c = 0.62) and air (0.24) but diminishes faster for electrolyte solution with time.

The velocity increases with increasing Eckert number (E_c), Magnetic parameter (M) but decreases with increase in rate of chemical reaction (K_c) for all the three fluids. Though, the effect of an increase in Grashof number is to raise the velocity values. Due to the presence of the magnetic field, it is observed that as time goes on, the velocity decreases for positive values of G_r but increases for negative values of G_r. However, the velocity remains positive for G_r>0 and negative for G_r<0.

REFERENCES

Abid, H., I. Khan, M.Z. Salleh and S. Sharidan, 2014. Slip effects on unsteady free convective heat and mass transfer flow with Newtonian heating. Therm. Sci., 20: 1939-1952.

Ali, M., M.A. Alim and M.S. Alam, 2014. Heat transfer boundary layer flow past an inclined stretching sheet in the presence of magnetic field. Int. J. Adv. Res. Technol., 3: 34-40.

Chaudhary, R.C. and P. Jain, 2006. Unsteady free convection boundary-layer flow past an impulsively started vertical surface with Newtonian heating. Rom. J. Phys., 51: 911-925.

Das, S., C. Mandal and R.N. Jana, 2012. Radiation effects on unsteady free convection flow past a vertical plate with Newtonian heating. Intl. J. Comput. Appl., 41: 36-41.

Etwire, C.J., Y.I. Seini and D.A. Azure, 2015. MHD thermal boundary layer flow over a flat plate with internal heat generation, viscous dissipation and convective surface boundary conditions. Intl. J. Emerging Technol. Adv. Eng., 5: 335-342.

Hussanan, A., M.Z. Salleh, I. Khan and R.M. Tahar, 2016. Heat and mass transfer in a micropolar fluid with Newtonian heating: An exact analysis. Neural Comput. Appl., 1: 1-9.

Hussanan, A., M.Z. Salleh, I. Khan, R.M. Tahar and Z. Ismail, 2015. Soret effects on unsteady MHD mixed convective heat and mass transfer flow in a porous medium with Newtonian heating. Maejo Intl. J. Sci. Technol., 9: 224-245.

Hussanan, A., M.Z. Salleh, R.M. Tahar and I. Khan, 2014. Unsteady boundary layer flow and heat transfer of a Casson fluid past an oscillating vertical plate with Newtonian heating. PloS One, 9: 1-9.

Martynenko, O.G., A.A. Berezovsky and Y.A. Sokovishin, 1984. Laminar free convection from a vertical plate. Intl. J. Heat Mass Trans., 27: 869-881.

Narahari, M. and M.Y. Nayan, 2011. Free convection flow past an impulsively started infinite vertical plate with Newtonian heating in the presence of thermal radiation and mass diffusion. Turkish J. Eng. Environ. Sci., 35: 367-378.

Seini, Y.I. and O.D. Makinde, 2013. MHD boundary layer flow due to exponential stretching surface with radiation and chemical reaction. Math. Prob. Eng., 2013: 1-7.

SeiniY, I., 2013. Flow over unsteady stretching surface with chemical reaction and non-uniform heat source. J. Eng. Manuf. Technol., 1: 24-35.

Siegel, R., 1958. Transient free convection from a vertical flat plate. Trans. Am. Soc. Mech. Eng., 80: 347-359.